Optical Properties of III–VI Lamellar Semiconductors Doped with Cu and Cd and of Related III–VI/Native Oxide Structures

Article *in* Journal of Nanoelectronics and Optoelectronics · December 2011

DOI: 10.1166/jno.2011.1203

CITATION
1

READS
153

8 authors, including:

Iuliana Caraman
University of Bacau
61 PUBLICATIONS **190** CITATIONS
SEE PROFILE

Liliana Dmitroglo
Moldova State University
15 PUBLICATIONS **12** CITATIONS
SEE PROFILE

L. Leontie
Universitatea Alexandru Ioan Cuza
124 PUBLICATIONS **2,052** CITATIONS
SEE PROFILE

V. Nedeff
University of Bacau
195 PUBLICATIONS **672** CITATIONS
SEE PROFILE

Journal of
Nanoelectronics and Optoelectronics
Vol. 6, 502–513, 2011

Optical Properties of III–VI Lamellar Semiconductors Doped with Cu and Cd and of Related III–VI/Native Oxide Structures

Silvia Evtodiev[1,*], Iulia Caraman[2], Liliana Dmitroglo[1], L. Leontie[3], V. Nedeff[2], A. Dafinei[4], G. Lazar[2], and I. Evtodiev[1]

[1] *Moldova State University, 60 A. Mateevici Str., Chisinau, MD-2009, Republic of Moldova*
[2] *Vasile Alecsandri University of Bacau, 157 Calea Marasesti, RO-600115 Bacau, Romania*
[3] *Alexandru Ioan Cuza University of Iasi, Bd. Carol I, Nr. 11, RO-700506 Iasi, Romania*
[4] *Faculty of Physics, University of Bucharest, Platforma Măgurele, Str. Fizicienilor nr. 1, CP Mg-11, Bucharest-Măgurele, RO-76900, Bucharest, Romania*

GaS, GaSe and GaTe are typical representatives of III–VI layered semiconductor materials, showing highly anisotropic mechanical and optical properties. At photon energies $h\nu < E_g$, the anisotropy ratio for the absorption coefficients at the $n = 1$ excitonic peak, corresponding to $\vec{E} \parallel \vec{C}$ and $\vec{E} \perp \vec{C}$ polarizations, is $\alpha_\parallel/\alpha_\perp \approx 15$. Optical functions $n_e(\lambda)$ and $n_o(\lambda)$ of GaS and GaSe in the wavelength range 0.36–22 μm have been determined. For the photon energies $h\nu < E_g^{ind}$, these correspond to a normal dispersion and can be described by power-law wavelength dependences. By means of FTIR transmission and reflection spectroscopy in the spectral range of 1000–85 cm^{-1}, for plan-parallel plates with thickness between several tens of nanometers and centimeters, the wavenumbers of longitudinal optical $\tilde{\nu}$(LO) and transverse optical $\tilde{\nu}$(TO) phonons have been determined for GaSe [$\tilde{\nu}_\perp$(LO) = 254 cm^{-1}, $\tilde{\nu}_\perp$(TO) = 214 cm^{-1}], GaS [$\tilde{\nu}_\perp$(LO) = 359 cm^{-1}, $\tilde{\nu}_\perp$(TO) = 297 cm^{-1}, $\tilde{\nu}_\parallel$(LO) = 336 cm^{-1}], and GaTe [$\tilde{\nu}$(LO) = 164 cm^{-1}, $\tilde{\nu}$(TO) = 118 cm^{-1}].

Keywords: Lamellar Semiconductors Undoped and Light-Doped (GaS, GaSe, GaTe)/Native Oxide, Anisotropy, Optical and Electrical Proprieties, Polarization, Exciton, Photon, Phonon TO and LO, Optical Functions, FTIR Spectrum, Reflection, Transmission, Absorption, Conductivity, Hall Concentration, Activation Energy, Mobility.

1. INTRODUCTION

The current research and development trends in photonics, nanoelectronics and optoelectronics are mainly determined by large area device application of divers classes of semiconductor nanomaterials. III–VI layered semiconductor compounds (in form of single crystals, thin films, nanowires and nanotubes, nanolamellas, nanoparticles, etc.), typical representatives of which are GaSe, GaS, InSe and GaTe, are considered among most promising materials for both fundamental and application research.[1–4] As a specific structural feature, these compounds display stratified packages of Chalcogen-Metal-Metal-Chalcogen type, the chemical bonds inside which have ionic-covalent nature, while between packages are of Van der Waals type.[5,6] The comparatively weak interaction between these packages favors easy cleavage of optically homogeneous plan-parallel layers of quite different thicknesses, up to nanometric. The anisotropy of the chemical bonding leads to specific mechanical and vibration properties,[7] as well as to a marked energy band anisotropy: the energy bandwidth along the C_6 crystallographic axis is much different in comparison with that within the plane of the stratified package.[8] Due to relative displacement of the atomic planes within the packages and of the packages itself, III–VI single crystals exhibit a large concentration of native defects, in the direction perpendicular to the C_6 axis.[9] Presence of native defects determines high stability of the optical, photoelectric and luminescent characteristics of GaSe and InSe-based devices under exposure to ionising radiations (γ, X) and high-energy particles (protons, neutrons).[10,11] The concentration of native defects in these materials is larger than that induced by doping and intercalation,[12–14] which results in low charge carrier

*Author to whom correspondence should be addressed.

 1555-130X/2011/6/502/012 doi:10.1166/jno.2011.1203

mobility and explains stability of their electric properties upon external excitations (high-energy radiations, small deformations, etc.).

Due to specific atomic arrangement in the crystal lattice, the valence bonds of chalcogens at the interface between stratified packages are practically compensated, which leads to weak cohesion between stratified packages, as well as low surface-state density and recombination rate values. These features, together with easy formation of native oxide (In_2O_3, Ga_2O_3) layers with high electric conductivity and optical transparency over a wide spectral range, strongly stimulate research of III–VI materials directed to photoreceiver and solar cell applications.[14–16]

In III–VI single crystals also manifest certain effects that can only be interpreted by taking into account the doping mechanism of crystal samples, influence of structural defects on the lattice vibration modes, as well as perturbation of electronic spectrum of the base material. Among these effects, formation of the exciton liquid in GaS crystals and emphasis of 2D electron gas in InSe by quantum Hall effect have been reported in Refs. [17 and 18], respectively.

The present work investigates the optical properties, over a wide spectral range, of layered materials GaS, GaSe, GaTe in form of single crystal lamellas, specially undoped and doped with Cu and Cd, as well as of nanolamellar III–VI/native oxide structures, from which the influence of dopant concentration and nature on the characteristics of electronic and phononic spectra of respective compounds was determined.

2. EXPERIMENTAL DETAILS

All GaS, GaSe and GaTe crystal samples have been grown by Bridgman technique, in a three-zone vertical furnace. High purity elements [Ga(5N), Se(4N), and spectrally pure S] have been used for the base materials synthesis, while highly pure elements [Cu(5N) and Cd(4N)] were used for doping purposes. Stoichiometric amounts of the base materials together with well-established amounts of dopants were placed in quartz ampoules (with internal diameter of 14–16 mm) which were pumped down to 10^{-5} Torr and tight closed, before being placed inside the oven, for synthesis. The temperature inside the furnace (metal compartment) was gradually increased up to 1100 °C, for GaS and GaSe, and 950 °C, in the case of GaTe, and maintained at the upper limit for 8 h and 10 h, respectively. To obtain single crystal samples, the ampoules containing melted material were proceeded through a 10 °C/cm temperature gradient zone, with a speed of 3 mm/h. After full melt solidification, the ampoules were cooled down to room temperature (oven disconnected), for 6–8 h. Additionally, single crystal samples were submitted to a thermal treatment at temperature 650–700 °C for 48 h.

From the bulk single crystals plan-parallel plates with area of 107 mm^2 and thickness ranging between ~40 nm and 0.5–0.7 cm have been split along the cleavage planes. They were used in optical measurements: transmission, for $\vec{E} \parallel \vec{C}$ and $\vec{E} \perp \vec{C}$ polarizations, and normal incidence reflection spectra, at temperatures from 78 K up to the room temperature. Native oxide layers (Ga_2O_3) at the surface of GaS and GaSe, as well as TeO_2–Ga_2O_3 onto GaTe, were obtained by heat treatment under normal ambient conditions, at 470 °C, for 30 and 90 min, respectively. At the same time, polycrystalline indium, gallium and tellur oxide layers were obtained by similar thermal treatments of respective metal films onto quartz substrates. TeO_2 lattice vibration bands were identified by using single crystal lamellas.

The optical transmittance (t) and reflectance (R) for normal light incidence on the (0001) surface of GaS, GaSe and GaTe single crystal lamellas, both unoxidized and covered by a native oxide layer, have been recorded in the spectral range of 200–900 nm by using a SPECORD M40 spectrophotometer with an energy resolution up to 1 meV. For oblique-incidence transmission measurements a goniometric device with high accuracy (of 30") was used. IR transmission and reflection spectra, in the wavenumber range of 7000–100 cm^{-1}, were registered with a FTIR-6300 spectrophotometer, equipped with accessories for easy measurement of single crystal and powder samples.

For Hall effect measurements, thin In films were evaporated onto (0001) surface of GaS, GaSe and GaTe single crystal lamellas and served as electrodes. The characteristics of both undoped and Cd and Cu-doped samples, as determined from Hall voltage measurements, are summarized in Table I.

The absorption coefficient in the C_6 axis direction ($\alpha_\perp$) has been determined from measurements of transmittance ($t_\perp$) and reflectance of single crystal lamellar samples with thickness (d) between 0.12 and 30 μm, by means of relation:[19]

$$t_\perp = \frac{(1-R)^2 \exp(-\alpha_\perp d)}{1-R^2 \exp(-2\alpha_\perp d)} \quad (1)$$

The absorption coefficient for the $\vec{E} \parallel \vec{C}$ polarization ($\alpha_\parallel$) has been determined from oblique-incidence [incident angle φ in respect with the normal to the (0001) plane] transmittance measurements.

The refractive indices ($n_\perp$ and $n_\parallel$) in the absorption domain ($\alpha d \leq 7$, $t \geq 10^{-3}$) were determined by using the interferential transmission spectra for normal incidence ($n_\perp$) and oblique incidence (at angle φ) with respect to the C_6 crystallographic axis, respectively. The following relation was used:

$$\lambda_m = 2n_\perp d/m \quad (2)$$

where $m = 1, 2, 3$.

Table I. Electric properties of GaS, GaSe and GaTe samples doped with Cu and Cd.

Sample	Conductivity type	Hall concentration (cm^{-3})	Activation energy (eV)	Mobility (cm^2V^{-1} s^1)
GaSe undoped	*p*	*p*-2.0×10^{14}	0.56	38–45
GaSe-0.01%Cd	*p*	*p*-2.0×10^{15}	0.24	20–35
GaSe-0.1%Cd	*p*	*p*-4.2×10^{15}	0.24	–
GaSe-0.2%Cd	*p*	*p*-5.7×10^{15}	0.24	–
GaSe-0.5%Cd	*p*	*p*-8.3×10^{15}	0.22	12–20
GaSe-0.05%Cu	*p*	3.0×10^{15}	0.13	45
GaSe-0.10%Cu	*p*	8.0×10^{15}	0.40–0.14	60–65
GaSe-0.10%Cu	*p*	3.0×10^{16}	0.11	54
GaS undoped	*n*	*n*-3.0×10^{13} ($T = 423$ K)	–	–
GaS-0.1%Cd	*n*	*n*-8.0×10^{13} ($T = 423$ K)	–	–
GaS-0.1%Cu	*n*	*n*-$(6.0–8.0) \times 10^{12}$ ($T = 423$ K)	–	–
GaTe undoped	*p*	8.0×10^{15}	–	40
GaTe-0.01%Cd	*p*	6.0×10^{16}	–	30–35
GaTe-0.01%Cu	*p*	8.5×10^{16}	–	40–50

The shape of the transmission spectrum at oblique incidence depends on the refractive index dispersion $[n_\perp(\lambda), n_\parallel(\lambda)]$ and is described by:[20]

$$m\lambda = n_\perp d\left[\left(1-\frac{\sin^2\varphi}{n_\perp^2}\right)^{1/2} - \left(1-\frac{\sin^2\varphi}{n_{II}^2}\right)^{1/2}\right] \quad (3)$$

where φ denotes the incidence angle.

The normal incidence absorption coefficient, taking into account interference influence in nanolamellar III–VI/(optically transparent) native oxide structures, is given by:[21]

$$\alpha = \frac{1}{d}\ln\left[\frac{-(1-R)(1-R_0)+\sqrt{(1-R)^2(1-R_0)^2+4R_0t^2}}{2R_0t}\right] \quad (4)$$

with

$$R_0 = \left(\frac{n_0-1}{n_0+1}\right)^2 \quad (5)$$

In the above equation, n_o is the refractive index of the oxide film, independently measured.

3. EXPERIMENTAL RESULTS

3.1. Refractive Index Dispersion

3.1.1. GaSe

A typical transmission spectrum of a plan-parallel GaSe plate in the wavelength range of 10–22 μm is shown in Figure 1.

The refractive index in the wavenumber interval $(\tilde{\nu}_m, \tilde{\nu}_{m+1})$ between two consecutive interference maxima (minima) is determined by using the relation:[22]

$$\tilde{n} = [2d(\tilde{\nu}_{m+1} - \tilde{\nu}_m)]^{-1} \quad (6)$$

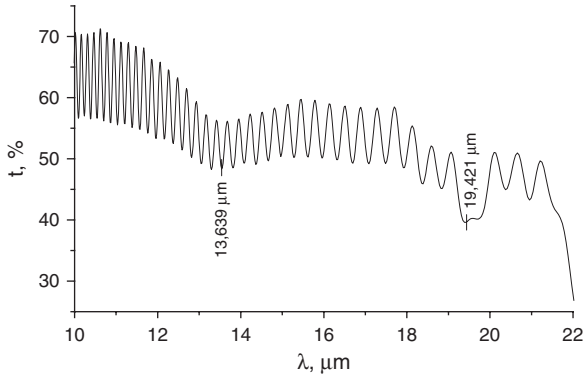

Fig. 1. Transmission spectrum of ε-GaSe lamella with thickness $d = 132$ μm.

where m represents the order of the interference band.

Using the recorded transmission spectra of plan-parallel plates with different thickness (d) ranged from 0.6 to 120 μm, the refractive index for wavenumbers within the optical transparency region of samples was determined.

Figure 2 presents spectral dependences of the ordinary (n_o) and extraordinary (n_e) refractive indices, in the wavelength range of 0.36–22 μm, for plan-parallel GaSe samples, both undoped (curves 4 and 4a) and doped with Cd (curves 5, 6 and 6a) and Cu (curves 7 and 7a). For comparison purposes, spectral curves $n_o(\lambda)$ and $n_e(\lambda)$ provided by Refs. [20, 23] (for the spectral range of 0.6–5 μm) and Ref. [24] (up to 18 μm) were plotted.

The dispersion of the refractive indices $n_o(\lambda)$ and $n_e(\lambda)$ in this spectral range is suitably described by the polynomial function

$$n_0^2(\lambda)\left[n_c^2(\lambda)\right] = A + B\lambda^{-2} + c\lambda^{-4} + D\lambda^{-6} + \Delta(\lambda) \quad (7)$$

where A, B, C and D denote constants. The correction $\Delta(\lambda)$ is used to give a better agreement with the experimental data in the vicinity of the absorption threshold of GaSe.

From this figure (curve 1) a sligth deviation of the curve plotted according to Eq. (7), with respect to the measured values can be observed at wavelengths $\lambda > 10$ μm. In this spectral range absorption bands of adsorbed gases and vapors onto sample surface or intercalated between stratified packages are also present. In order to minimize the influence of the adsorbed gases on the recorded data, the measured lamellar samples were submitted to a vacuum (10^{-4} Torr) light annealing at 120–140 °C.

Magnitude of refractive indices n_o and n_e in the spectral region of phononic bands was confirmed by measurements using a fixed wavelength, according to the method reported in Ref. [25]. This method allows to avoid the influence of interference effects on the impurity and multiphononic absorption bands. In order to perform these experiments, a monochromatic light beam with wavelength of 22.9 μm was selected from the emission spectrum of an IR radiation source with temperature of ~1600 °C, by means

of a Ge interferential filter ($\Delta\lambda \approx 0.8$ μm). $\vec{E} \parallel \vec{C}$ and $\vec{E} \perp \vec{C}$ polarizations of the incident light were obtained by using a transmission diffraction polarizer. The angle of incidence on the sample surface was measured by a GS-5 type goniometer with accuracy of 5′. As can be observed from Figure 2, the obtained values of n_o and n_e at this wavelength are in good agreement with those determined from the interferential transmission spectrum.

Cd and Cu-doping of GaSe, at concentrations $c \leq 1$ at.% [Fig. 2, curves (4–7 and 4a–6a)], practically doesn't change the dispersion law for n_o and n_e at wavelengths $\lambda > 2$ μm. For this doping range a relatively small increase in their values is registered in the region of the fundamental absorption edge of GaSe. In this spectral region exciton interaction with impurity atoms manifest itself more pronouncedly, together with optical electron transitions from shallow acceptor levels to the conduction band.

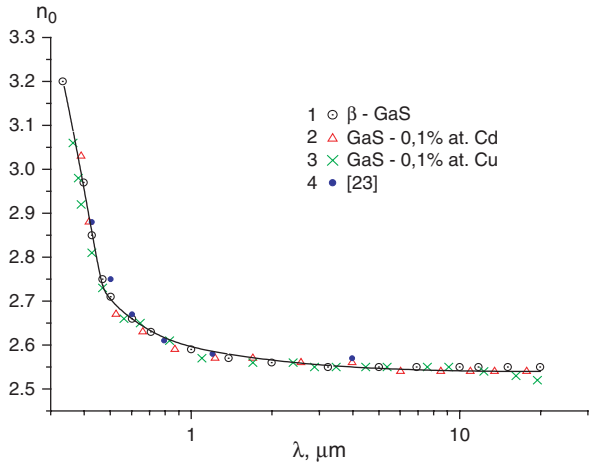

Fig. 3. Spectral dependence of the refractive index n_0 for GaS single crystals, undoped (1) and 0.1 at.% doped with Cd (2) and Cu (3).

3.1.2. GaS

Transmission spectra of GaS lamellas with thickness $d \leq 70$ μm display an interferential character for wavelengths up to $\approx$20 μm. But in the spectral range $\lambda > 20$ μm, the interference bands are seen to overlap with phononic and impurity absorption bands. The refractive index dispersion of GaS lamellas, both undoped and lightly-doped ($c = 0.1$ at.%) with Cu and Cd is presented in Figure 3.

The $n(\lambda_o)$ characteristic in the wavelength rage of 330 nm–20 μm, for both undoped and slightly doped GaS samples, is suitably described by the following polynomial function:

$$n(\lambda) = A + \frac{B}{\lambda^2} + \frac{C}{\lambda^4} + \frac{D}{\lambda^6} \qquad (8)$$

with $A = 2.548$; $B = 0.0279$; $C = 3.321 \times 10^{-3}$ and $D = 4.213 \times 10^{-4}$, and λ in μm.

Deviation of experimental data with respect to the curve (8), emphasized in the range $\lambda < 0.390$ μm, is produced by the influence of the optical transitions taking place in the vicinity of the M point of the Brillouin zone.[26]

3.2. Fundamental Optical Absorption $h\nu \geq E_g$

3.2.1. GaSe

The absorption coefficient (α) of plan-parallel lamellas with thickness d was determined by using transmission and reflection spectra registered for normal incidence light. In Figure 4(a) spectral dependences $\alpha(h\nu)$ of GaSe crystals at room and liquid nitrogen temperatures are shown.

In the region of fundamental absorption edge, at 293 K (curve 1), a narrow band of $n = 1$ exciton absorption with maximum at $E_{ex}(n = 1) = 2.013$ eV is emphasized. The absorption coefficient at the peak of this band is of $\sim$1700 cm^{-1}. For decreased sample temperature down to

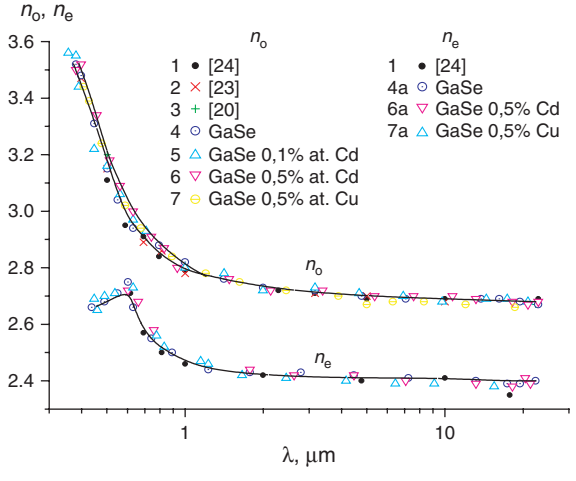

Fig. 2. Dispersion of the refractive indices n_0 and n_e for specially undoped (4, 4a) and doped GaSe single crystals with Cd [0.1 at.%-(5);0.5 at.%-(6, 6a)] and Cu [0.5 at.%-(7, 7a)].

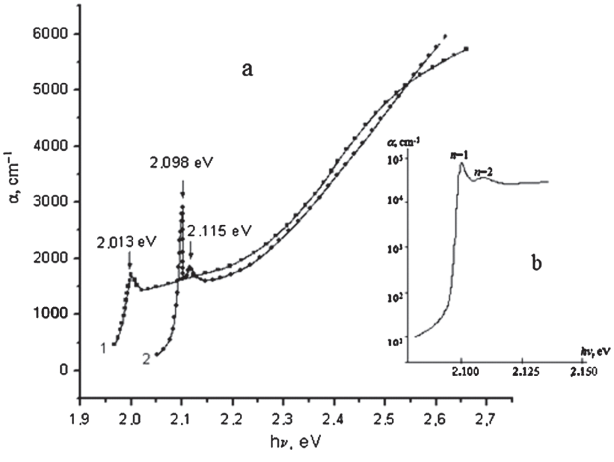

Fig. 4. Absorption spectra of GaSe single crystals. (a) $\vec{E} \perp \vec{C}$ polarization, at temperatures 393 K (curve 1) and 78 K (curve 2); (b) $\vec{E} \parallel \vec{C}$ polarization, at temperature 78 K.

78 K (curve 2), the width of the exciton band monotonically decreases, while the absorption coefficient at the band center is seen to increase up to 2900 cm^{-1}. Besides, a blue shift of the exciton absorption band can be observed. The temperature dependence of the exciton peak energy position is well described by:[27]

$$E_{exc}(T) = E_{exc}(0) - \frac{\alpha T^2}{T+\beta} \quad (9)$$

with $E_{ex}(0) = 2.134$ eV, $\alpha = 2.33 \times 10^{-4}$ eV/K and $\beta = -38.5$ K.

At temperature $T = 78$ K, together with $n = 1$ exciton line (energy $E_{n=1} = 2.098$ eV), the $n = 2$ exciton band, peaked at $E_{n=2} = 2.115$ eV, is also clearly emphasized.

Using the mentioned peak energy positions for $n = 1$ and $n = 2$ excitons the forbidden bandwidth at 78 K and excitonic Rydberg in GaSe were determined and were found to be $E_g = 2.121$ eV and $R_o = 22.6$ meV.

If one assumes that in temperature range of 78–293 K the binding energy of the electron–hole pair remains constant, then the forbidden bandwidth of GaSe, at $T = 293$ K, is $E_{ex}(n = 1) + R_o = 2.035$ eV. Besides discrete exciton spectrum, at energies $h\nu > E_g$, the excitonic continuum region is present, where $n > 2$ lines are seen to overlap.

In the depth of the fundamental absorption band, the absorption coefficient increases monotonically with energy at both temperatures 293 and 78 K, and reaches its maximum, of ~5200 cm^{-1}, at photon energy $h\nu = 2.55$ eV. Own to the specific layered structure, GaSe single crystals exhibit high anistropy in the mechanical properties, which is also manifested in their electric and optical properties.

In Figure 4b the absorption spectrum of GaSe for the $\vec{E} \parallel \vec{C}$ polarization, at $T = 78$ K, is presented. As can be observed from Figures 4(a) (curve 2), and 4(b) the anisotropy of the optical absorption is more pronounced in the domain of the direct optical transitions (range of the exciton continuum) and direct excitons.

At temperature 78 K, for both polarizations, $n = 1$ and $n = 2$ electron–hole bounds are created.

The ratio of absorption coefficients at the maximum of $n = 1$ exciton line, for $\vec{E} \parallel \vec{C}$ and $\vec{E} \perp \vec{C}$ polarizations, is equal to 17, which is in good accordance with the anisotropy coefficient of the effective mass, equal to 16.[28]

3.2.2. GaSe:Cu

Optical absorption in the region of the absorption edge and in the depth of the fundamental absorption band of single-crystalline GaSe lamellas doped with Cu in the concentration range from 0.005 at.% up to 0.50 at.%, at temperatures 293 K and 78 K, was investigated (Fig. 5).

As can be inferred from the comparison of curves 1 from Figures 4 and 5, the fundamental absorption edge of specially undoped GaSe single crystals practically coincides with that of light-doped (0.005 at.%Cu) samples, for

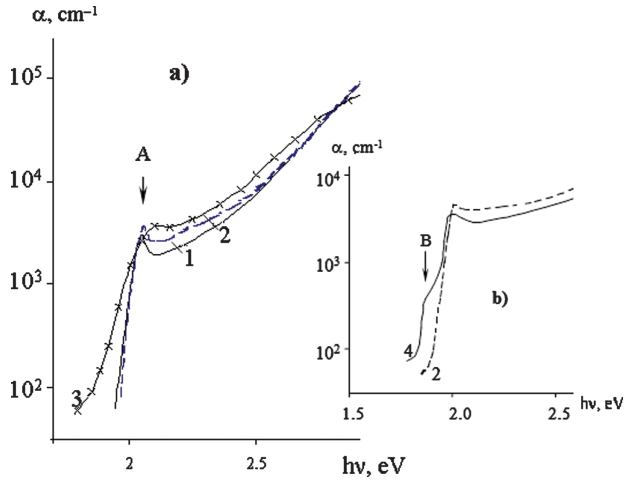

Fig. 5. (a) Spectral dependence of the absorption coefficient, at 78 K, for Cu-doped GaSe crystals. 1—0.005 at.%; 2—0.01 at.%; 3—0.50 at.%. (b) Absorption spectrum of GaSe crystals doped with Cd. 2—0.05 at.% and 4—0.50 at.%.

absorption coefficients in the range of $10^2 - 10^3$ cm^{-1}. In this spectral region, the slope of $\alpha(h\nu)$ curves exhibits a decreasing tendency together with increased Cu doping concentration. In the case of GaSe:Cu (0.50 at.%) single crystals, the fundamental absorption edge is determined by direct optical transitions between ionized Cu acceptor levels and the conduction band. The energy interval corresponding to the mentioned transitions (Fig. 6) is equal to 1.89 eV. Taking into account that the band gap of ε-GaSe crystals, at 293 K, is of ~2.035 eV, the energy of Cu impurity level was determined and found to be 0.14 eV with respect to the valence band top.

In the region of fundamental absorption edge of GaSe lamellas doped with 0.50 at.% Cd, besides particularities that are characteristic to undoped crystals, a threshold (B, Fig. 5(b)) is emphasized, located at 1.95 eV. Since this particularity is not present in the case of other dopants (Cu, Sn),[29] one can admit that the fundamental absorption edge in the 0.50 at.% Cd-doped GaSe samples is formed by the merging of the Cd impurity band (high energy side) with the fundamental absorption edge of GaSe. Knowing the direct band gap of gallium selenide and the energy position of the Cd impurity band, the energy of the acceptor level induced by Cd atoms, with respect to the valence band top, was determined and found to be 90 meV.

3.3. Optical Absorption in the Region $h\nu < E_g$

3.3.1. GaSe, GaSe:Cd, GaSe:Cu

Impurity atoms and native structural defects engender a wide range of localized discrete levels in the semiconductor band gap, through which electron transitions take place, which determine optical, electric, luminescent and photoelectric properties of respective material. The shape of the

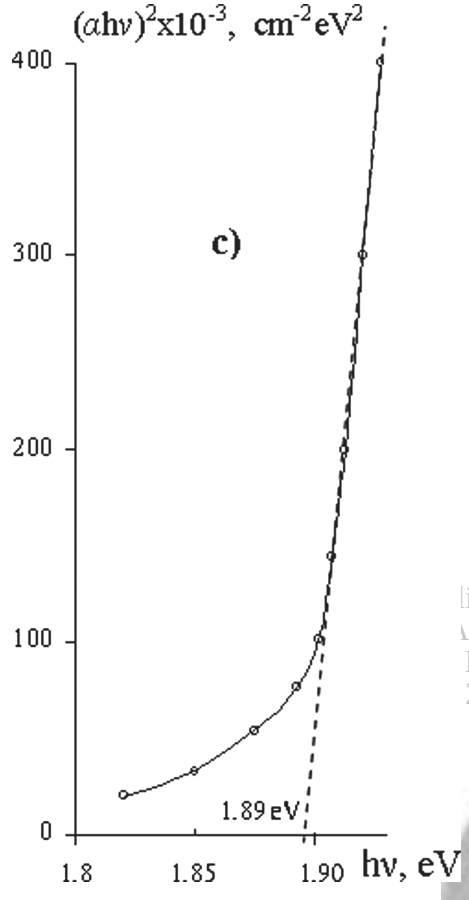

Fig. 6. Spectral dependence of the absorption coefficient in the impurity absorption range of GaSe single crystals doped with 0.50 at.% Cu.

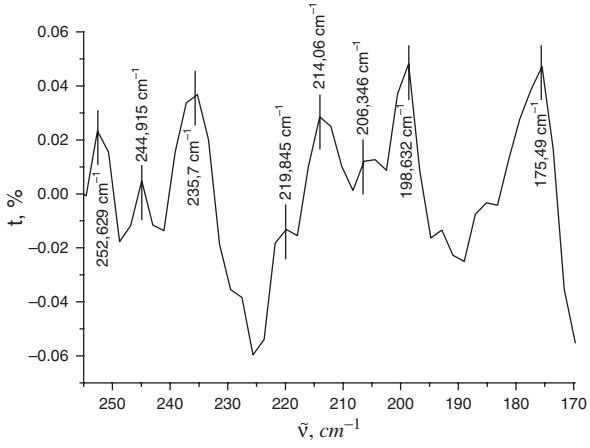

Fig. 8. Second derivative of the optical transmission spectrum in the region of monophonon vibrations of the single-crystalline ε-GaSe plate with thickness of 2.5 μm.

optical spectra of III–VI layered compounds, in the energy range $h\nu < E_g$, is determined, besides own crystal lattice vibrations (characteristic to perfect crystals), by the presence of native structural defects and of those induced by sample doping.

In Figure 1(a) fragment of the transmission spectrum of a GaSe plate, 130 μm thick, in the spectral range of 10–27.5 μm, was represented. In the mentioned wavelength range the interferential character of the spectrum is influenced by diphonon (band 4) and impurity absorption bands, peak positions of which are given in Table II.

In the wavelength range between 100 and 600 cm^{-1}, in transmission spectrum of the micronic plates (about 2.5 μm thick) (Fig. 7) the absorption band of TO phonons [$\tilde{\nu}$(TO) = 214.06 cm^{-1}] is clearly emphasized. The particluarities of complex structure of transmission spectrum may be easy observed in the case of second derivative spectrum ($d^2t/d\tilde{\nu}^2$) in Figure 8.

The layered structure of GaSe single crystals leads to a well marked anisotropy of reflectance (Fig. 2), exciton absorption (Fig. 4), as well as of the vibration spectrum. The maxima of the $(d^2t/d\tilde{\nu}^2)(\tilde{\nu})$ spectrum correspond to phonon wavenumbers. In this way, from Figure 8 LO and TO phonons in $\vec{E}\perp\vec{C}$ polarization can be identified [$\tilde{\nu}_\perp$(LO) = 252.63 cm^{-1} and $\tilde{\nu}_\perp$(TO) = 214.06 cm^{-1}], together with several relevant bands [$\tilde{\nu}_1$ = 244.92 cm^{-1}, $\tilde{\nu}_2$ = 235.70 cm^{-1}, $\tilde{\nu}_3$ = 219.84 cm^{-1}, $\tilde{\nu}_4$ = 206.35 cm^{-1}, $\tilde{\nu}_5$ = 198.63 cm^{-1}, and $\tilde{\nu}_6$ = 175.49 cm^{-1}]. In Ref. [30] it has been demonstrated that in the absorption spectra of layered III–VI materials, in particular GaS, besides vibration bands in the $\vec{E}\perp\vec{C}$ polarization, vibration sub-bands in the $\vec{E} \parallel \vec{C}$ polarization also occur.

Certain absorption bands lying in this spectral region can be ascribed to γ-GaSe polymorph

Table II. Wavenumbers for the diphonon, multiphonon and impurity bands in ε-GaSe lamellas.

N/o	$\tilde{\nu}$ (cm^{-1})
1	375.08
2	389.55
3	404.97
4	420.40
5	434.86
6	447.40
7	479.22
8	489.83
9	511.04
10	539.97
11	616.14
12	720.28
13	1042.3
14	1444.4
15	1589.0
16	2347.9
17	2854.1
18	2925.4
19	3340.1
20	4752.7
21	6026.5

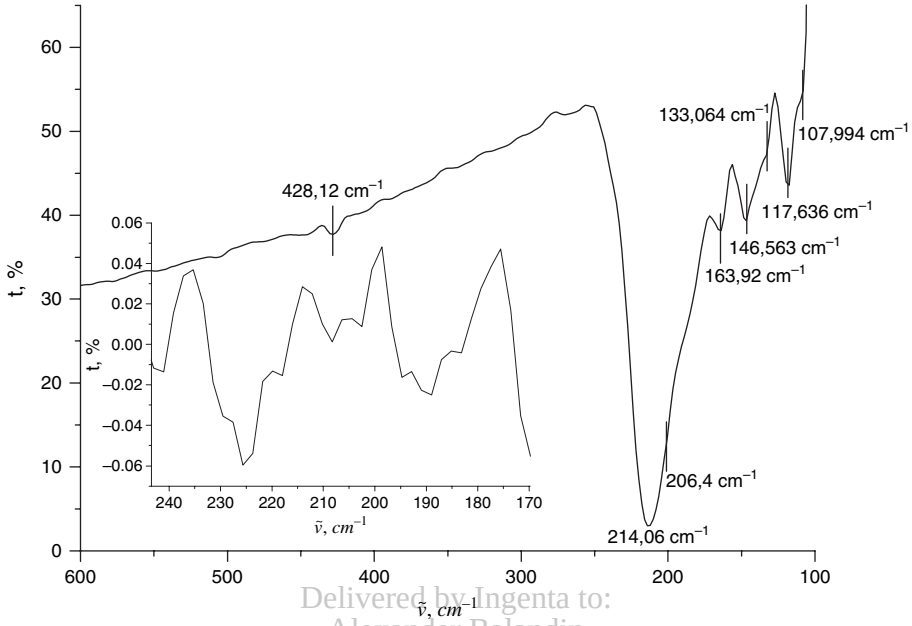

Fig. 7. Spectral dependence of transmittance $t(\tilde{\nu})$ for a 2.5 μm thick GaSe plate.

(e.g., $\tilde{\nu}_2 = 235.7$ cm^{-1} and $\tilde{\nu}_1 = 245.0$ cm^{-1}).[31] Besides, a low-intensity diphonon band $[2\tilde{\nu}(\mathrm{TO}) = 428.12$ cm$^{-1}]$ and several impurity monophonon absorption bands located in the range $\tilde{\nu} < 200$ cm^{-1} are also registered. The intensity ratio for the monophonon and diphonon absorption bands is $I_{\tilde{\nu}(\mathrm{TO})}/I_{2\tilde{\nu}(\mathrm{TO})} \approx 36$. Because ε-GaSe unit cell doesn't have an inversion centre, the alternative selection rules allow presence of lattice vibration bands in the IR absorption and Raman spectra. For this reason, the threshold at $\tilde{\nu} \approx 133.06$ cm^{-1} may be ascribed to the symmetric vibrations inside stratified crystal package with respect to the vertical plane, which is active in the case of Raman spectra.[31]

As can be observed in Figure 8, in the wavelength range below absolute minimum of $\tilde{\nu}_{\mathrm{TO}}$ band, a second monophonon band, located at 206.4 cm^{-1} is emphasized. In this spectral range vibration of atomic planes and optical transitions between the valence band and ionized acceptor levels and between donor levels and the conduction band pronouncedly manifest. The positions of these particularities and the energies of the impurity levels, responsible for the complex structure of transmission spectrum in the range of 1000–100 cm^{-1} are given in Table III.

In the wavelength range of 19–20 μm, the transmission spectrum (Fig. 1) exhibits an absorption band with complex structure. Besides interference effects, $t(\lambda)$ spectrum is also perturbed by other absorption mechanisms. The particularities of the absorption band lying in the range of 13.7 μm–16.7 μm have been established by analyzing spectral transmittance of plan-parallel samples, for which interference phenomena don't occur. As can be seen in Figure 9, this band is composed by at least three bands, two of which ($3\tilde{\nu}^{l}_{\mathrm{TO}} = 644$ cm^{-1} and $3\tilde{\nu}^{ll}_{\mathrm{TO}} = 620$ cm^{-1}) correspond to the triphonon absorption.

Table III. Wavenumbers of monophonon and impurity absorption bands in GaSe crystals.

N/o	$\tilde{\nu}$ (cm^{-1})	$h\nu$ (meV)
1	166	21.0
2	207 [$\tilde{\nu}_{\parallel}$(TO)]	25.7
3	194	24.0
4	150	18.6
5	143	17.7
6	119	14.8
7	108	13.4

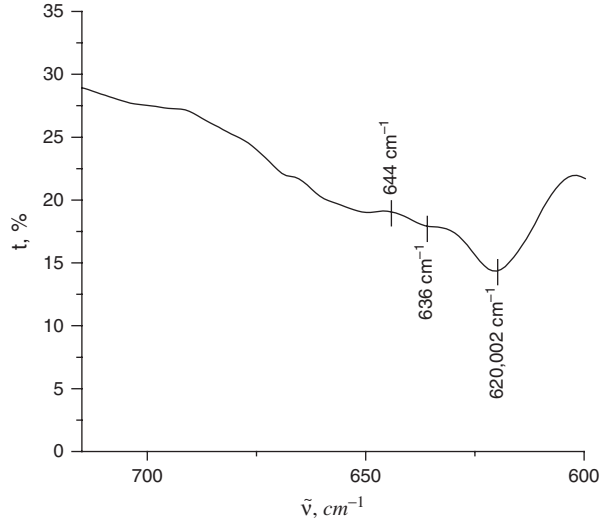

Fig. 9. Transmission spectrum of single crystal GaSe plate ($d \approx 1.3$ cm).

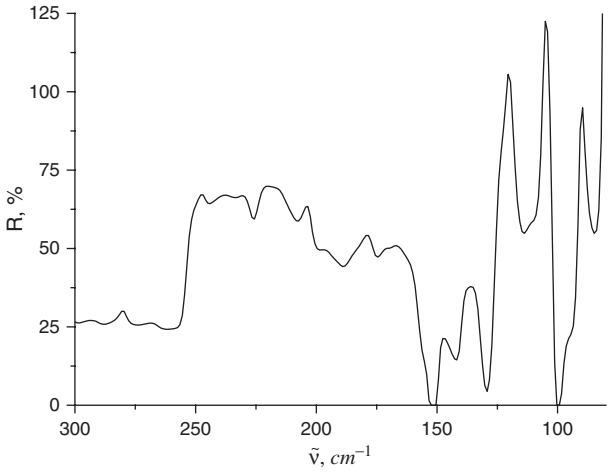

Fig. 10. Reflection spectrum of the gallium oxide film on quartz.

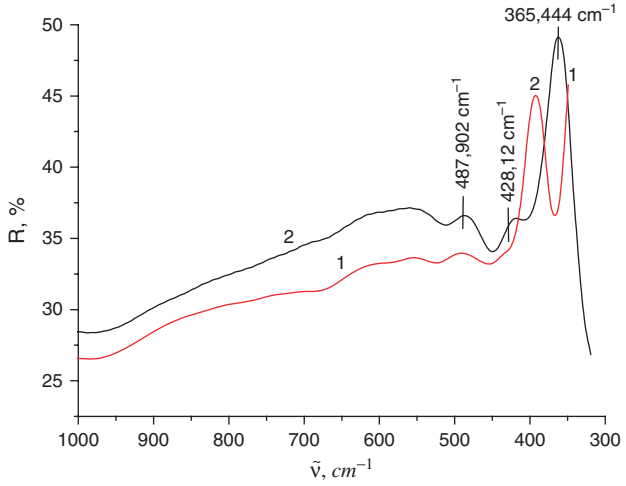

Fig. 11. Reflection spectra of GaSe lamella, prior to (curve 1) and after 90 min annealing at 470 °C, in ambient atmosphere (curve 2).

3.4. IR Absorption and Reflection Spectra of Nanolamellar GaSe/Native Oxide Structures

3.4.1. GaSe–Ga_2O_3

In the case of long-term preservation, as well as of thermal treatment under normal ambient conditions, surface of lamellar III–VI materials is covered by a native oxide layer.[14, 32, 33]

In_2O_3 and Ga_2O_3, native oxides of Inse and GaSe respectively, exhibit high optical transparency in a wide spectral range, from the UV frontier, up to near-IR, as well as electric conductivity. Besides, during the oxidation process of the semiconductor surface certain changes in the structure of localized energy levels in the forbidden band of the base material do occur.

As a result of long-term oxidation of lamellar GaSe, under ambient (presssure and temperature) conditions, several oxides [GaO, Ga_2O_3, Ga_2O_2, SeO, SeO_3, SeO_4, Se_2O_5, $Ga_2(Se_2O_5)_3$] may be formed, in different proportions, at the semiconductor surface.[15, 34] In order to identify the nature of the surface oxide formed by heat treatment, FTIR reflection spectra of the single crystal GaSe plate and a gallium film deposited on quartz (SiO_2) support, both annealed at 450 °C in ambient atmosphere, have been recorded. FTIR reflection spectrum (Fig. 10) of the oxidized Ga film onto quartz contains several vibration bands that can be ascribed to β-Ga_2O_3; these were also determined by Raman spectroscopy.

Figure 11 presents a typical reflection spectrum of a plan-parallel GaSe sample, before (curve 1) and after thermal oxidation for 90 min, at 470 °C (curve 2).

In the spectral range of 300–1000 cm^{-1} the $R(\tilde{\nu})$ spectrum of freshly cleaved GaSe layer contains three reflection bands: a high-intensity one, peaked tat 365 cm^{-1} and two much weaker bands at 420 cm^{-1} and 485 cm^{-1}. As a result of heat treatment at 470 °C for 30 min, in open atmosphere, the intense band is seen to attenuate, but a new high-intensity band is formed at 390 cm^{-1}.

Dynamics of forming the reflection band of the native oxide layer (Ga_2O_3) onto (0001) GaSe surface is illustrated by curve 2 (Fig. 10). Therefore, one can admit that the band at 365 cm^{-1} is determined by the presence of adsorbed gas molecules on the surface of GaSe lamella, which can be eliminated by heat treatment.

In Figure 12 fragments of the reflection spectra of (0001) GaSe single crystals prior (a) to and after 90 min thermal oxidation (b), performed at 470 °C in ambient atmosphere are illustrated. In the spectral region of 260–190 cm^{-1} a prominent reflection band is observed, the contour of which is typical for the monophonon reflections.[35]

Reflection bands with similar contours were also reported for cubic-symmetry crystals, like GaAs[36] and InAs.[37] By analysing the structure of the mentioned band wavenumbers of fundamental LO and TO phonons have been determined and found to be $\tilde{\nu}_{\perp}(LO) = 256.5$ cm^{-1} and $\tilde{\nu}_{\perp}(TO) = 214.1$ cm^{-1}, respectively, in good agreement with the values provided by Ref. [31].

As can be inferred from Figure 11, the main particularities of the $R(\tilde{\nu})$ spectrum are maintained in the case of (0001) surface covered by a native oxide layer. The noncoincidence between energies of vibration bands of GaSe transmission (Table V) and reflection spectra (Table IV) is caused by the influence of the adsorbed gases on the lamella surface.

Characteristic to Ga_2O_3 native oxide layers onto (0001) GaSe surface and onto quartz is presence of certain intense bands lying in the region of monophonon vibrations, located at 104, 115 and 131 cm^{-1}.

The reflection spectrum of oxidized GaSe surface contains, besides characteristic bands of GaSe lattice vibrations, a series of new bands (122 cm^{-1}, 137 cm^{-1}, 166 cm^{-1}), corresponding to the gallium oxide vibrations. The wavenumbers of interplanar and atomic plane vibrations are listed in Table IV.

Table IV. Energies (in cm^{-1}) of the vibration bands (Fig. 11) of the reflection spectra for the (0001) GaSe surface of a freshly cleaved, 35 μm thick plate, $\tilde{\nu}_1$, and after annealing at temperature 470 °C, for 90 min, $\tilde{\nu}_2$.

N/o	$\tilde{\nu}_1$ (cm^{-1})	N/o	$\tilde{\nu}_2$ (cm^{-1})	Interpretation
1	83	1	–	Native oxide
2	93	2	94	GaSe
3	100	3	100	GaSe
4	110	4	111	GaSe
5	114	5	122	
6	128	6	137	
7	142	7	142	GaSe
8	151	8	152	GaSe
9	174	9	166	
10	189	10	175	GaSe
11	200	11	198	
12	208	12	219	
13	214.06	13	231	
14	226	14	–	
15	243	15	244	GaSe
16	261.3	16	260 [$\tilde{\nu}$(LO)]	
17	273.8	17	292	

As can be inferred from this table, frequencies of TO phonnos [($\tilde{\nu}_{TO} = 214$ cm^{-1})] and of low-energy phonnos (105 cm^{-1} and 90 cm^{-1}), which are determined by the vibrations of the atomic planes against each other, remains unchanged, within the limit of experimental errors.

Formation of gallium oxides occurs by O substitution of Se atoms from the surface of stratified GaSe packages. This substitution leads to weakening of the valence bonds in the direction of the C_6 axis, as well as of strong ionic-covalent bonds between the atoms inside the GaSe packages. This structural changes, together with the presence of complimentary oxides (GaO, Ga_2O), lead to decrease in the vibration frequencies at the sample surface.

3.4.2. GaS and GaS/Native Oxide

A typical reflection spectrum of a plan-parallel GaS plate, 35 μm thick, in the spectral range from 450 cm^{-1} up to 100 cm^{-1}, is presented in Figure 13.

In the examined spectral range presence of the fundamental LO[$\tilde{\nu}_\perp$(LO) = 360 cm^{-1}] an TO[$\tilde{\nu}_\perp$(TO) = 297 cm^{-1}] phonons is clearly observed. Identification of the fundamental TO phonon, for the polarization perpendicular to the C_6 axis, has been made in Ref. [30] by analysing the absorption spectrum of a GaS layer with submicronic thickness, in the spectral range of 260–360 cm^{-1}. From the analysis of the respective contour and of incidence angle dependence of this band intensity for the (0001) GaS surface, in Ref. [38] has been found that the band at 297 cm^{-1} is produced by resonant light absorption with formation of TO phonons in $\vec{E}\perp\vec{C}$ polarization, with energy $\tilde{\nu}_\perp$(TO) = 297 cm^{-1}. At the ame time, a series of narrow contour bands is evidenced in the mentioned spectral range, which correspond to the vibrations of the atomic plane assemblies and diphonon combinations. Energies of these vibrations are given in Table V.

$R(\tilde{\nu})$ spectra being registered at oblique incidence (an incidence angle of 30° with respect to the C_6 axis), within the monophonon reflection band a mimimum at 336 cm^{-1}

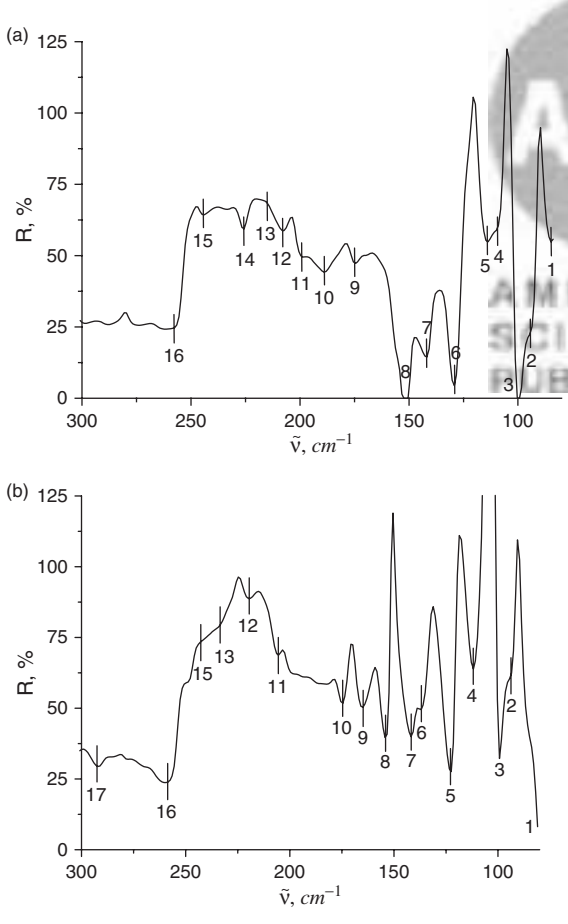

Fig. 12. FTIR reflection spectra of the freshly cleaved GaSe surface (a) and after oxidation at temperature 470 °C, for 90 min (b).

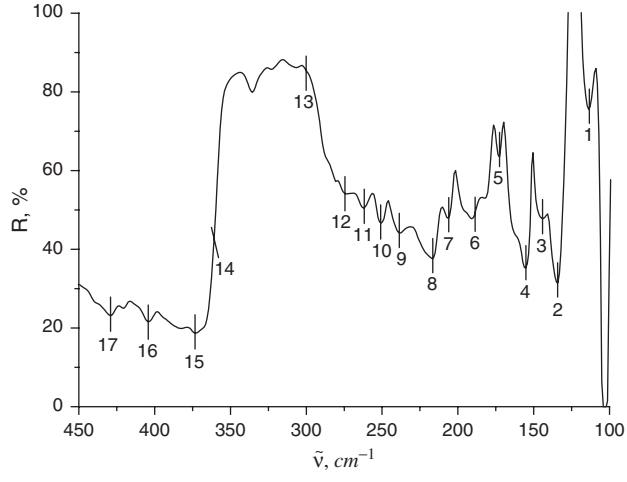

Fig. 13. Reflection spectrum of (0001) surface of single crystal GaS layer wit thickness of 35 μm, for oblique-light incidence, of 30 °C, with respect to the C_6 axis.

Table V. Energies of monophonon lattice vibrations, of atomic plane assembly vibrations and of elementary vibration combinations, determined from the reflection and transmission (bands nos. 18-21) spectra of GaS plate with thickness of 3.5 μm.

N/o	A $\tilde{\nu}$ (cm^{-1})	N/o	B $\tilde{\nu}$ (cm^{-1})	Interpretare
1	113.5	1	649	
2	133.8	2	637	
3	143	3	595	
4	154	4	480	
5	173	5	434	
6	188.5	6	422	Raman active
7	206.5	7	400	
8	216.5	8	392	$\tilde{\nu}_8$
9	239	9	386	
10	250	10	377	
11	262			
12	273			
13	297			$\tilde{\nu}_\perp$(TO)
14	360			$\tilde{\nu}_\perp$(LO)
15	377			
16	406			
17	433			$2\tilde{\nu}_8$
18	423			
19	478			$2\tilde{\nu}_9$
20	592			$2\tilde{\nu}_\perp$(TO)
21	637			$2\tilde{\nu}_\parallel$(TO)

and a maximum at 317 cm^{-1} are emphasized. The registered minimum on the monophonon band contour is ascribed in Ref. [30] to LO vibrations in the $\vec{E} \parallel \vec{C}$ polarization, while the maximum is in good agreement with the energy of TO phonons for the same polarization.[39]

In the spectral region of 12–27 μm, diphonon absorption bands (Fig. 14) are present, energies of which (in cm^{-1}) are listed in Table V. The absorption minima located at $\lambda_1 = 15.7$ μm ($\tilde{\nu}_1 = 637$ cm^{-1}) and $\lambda_2 = 16.9$ μm ($\tilde{\nu}_2 = 592$ cm^{-1}) are in good agreement with the energies of two TO phonons [$2\tilde{\nu}_\parallel$(TO) and $2\tilde{\nu}_\perp$(TO)] in the $\vec{E} \parallel \vec{C}$ and $\vec{E} \perp \vec{C}$ polarizations, respectively. The high-intensity band with maximum at $\lambda_3 = 26.5$ μm ($\tilde{\nu}_3 =$ 377 cm^{-1}) (Fig. 14), which is found in the reflection spectrum as a low-intensity minimum, represents a two-phonon $\tilde{\nu}_6 = 188.5$ cm^{-1} summation (respective phonon is well pronounced in the reflection spectrum).

The reflection spectrum of the GaS plate with thickness of 35 μm, thermally oxidized at 450 °C for 30 min, displays (Fig. 15), in the spectral region of 20–27 μm (500–350 cm^{-1}), several bands characteristic of Ga_2O_3 ($\tilde{\nu}_4 = 400$ cm^{-1}, $\tilde{\nu}_3 = 410$ cm^{-1}, $\tilde{\nu}_2 = 424$ cm^{-1} and $\tilde{\nu}_1 =$ 434 cm^{-1}). Therefore, one can state that (0001) surface of GaSe and GaS lamellas is covered by thermal treatment, at 450–470 °C, by a native oxide, Ga_2O_3, layer.

3.4.3. GaTe, GaTe/Native Oxide

In Figures 16(a and b) FTIR reflection spectra of the natural surface of a GaTe plate with thickness of 55 μm, cleaved from the bulk single crystal, are presented.

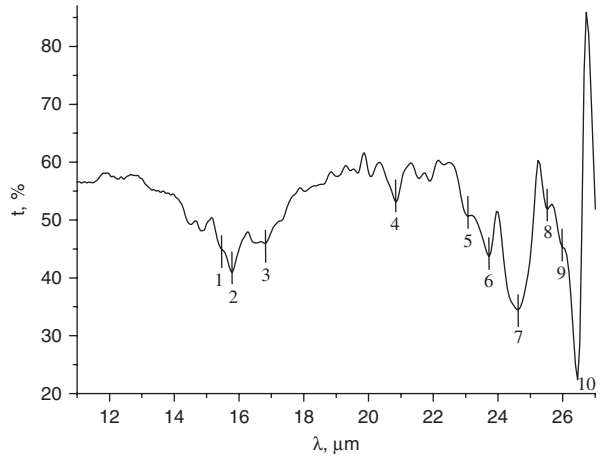

Fig. 14. Transmission spectrum of single crystal GaS plate.

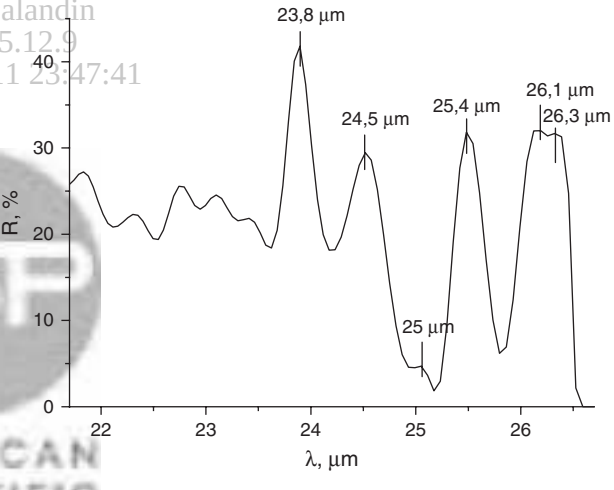

Fig. 15. Reflection spectrum of (0001) GaS surface of a 35 μm thick plan-parallel plate, annealed for 30 min at 450 °C.

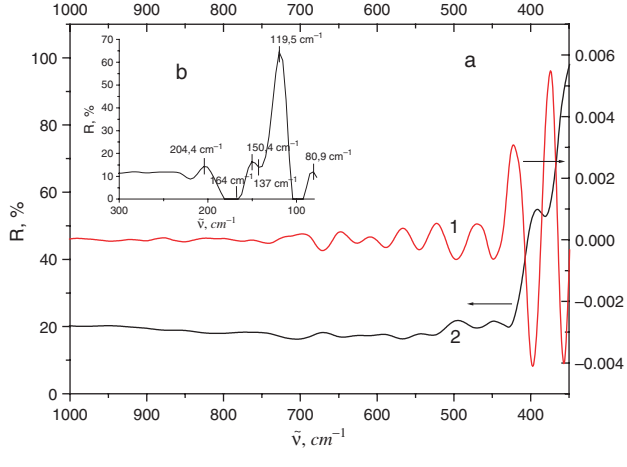

Fig. 16. Reflection spectrum of a GaTe plate, 55 μm thick, prior to (curve 1) and after annealing at temperature 470 °C for 90 min (curve 2), in the spectral region of 1000–950 cm^{-1} (a) and 80–300 cm^{-1} (b).

Table VI. Wavenumbers for the reflection maxima of TeO_2 surface covered by a native oxide layer, in the spectral range of 100–400 cm^{-1}.

N/o	$\tilde{\nu}$ (cm^{-1})
1	397.2
2	350.9
3	279.6
4	254.5
5	222.7
6	188
7	171.6
8	154.2
9	138.8
10	126.3
11	119.5
12	103

As it can be observed, in the spectral region of 1000–350 cm^{-1} a series of reflection bands is emphasized. The low intensity of the reflection bands lying between 670 and 450 cm^{-1} is an indicative of their multiphonon character. The reflection band lying in the range of 164–94 cm^{-1} (Fig. 15(b)), own to its contour shape and large magnitude of the reflectance (~65%), may be attributed to monophonon reflection with the wavenumber $\tilde{\nu}(TO) = 119.5$ cm^{-1}. The wavenumber of LO vibrations could be of 164 cm^{-1}. In order to elucidate nature of the band at 137 cm^{-1} (Table IV), supplementary studies of reflection spectra in polarized light and Raman diffusion are necessary.

The surface of GaTe plates, thermally treated for 30–90 min at tempeature 470 °C, is covered by a white colour layer, which may contain several gallium and tellurium oxides. These oxides are all optically transparent in the near-UV-vis region, instead, Ga_2O_3 is a good electric conductor, while TeO_2 is a good dielectric material. In order to establish composition of the oxide layer at the surface of GaTe plate, the reflection spectrum of this surface, in the spectral range from 100 up to 480 cm^{-1} has been recorded (Fig. 17). The peak positions of the corresponding reflection bands are listed in Table VI.

The comparative analysis of the $R(\tilde{\nu})$ spectrum of both unoxidized and oxidized GaTe layers reveals that the oxide layer at the surface of GaTe perturbs the structure of its mutiphonon spectrum. At wavenumbers $\tilde{\nu} < 440$ cm^{-1} (Fig. 16(b)) an intense reflection band is present, which, as can be inferred from Figure 17, corresponds to Te–O vibrations in TeO_2 single crystals.

The structure of the reflection spectrum of the oxidized GaTe surface, in the range of 250–80 cm^{-1}, is determined by monophonon reflection in GaTe substrate and reflection of TeO_2 layer at the surface of GaTe. Therefore, as a result of thermal oxidation, in ambient atmosphere, of III–VI lamellar materials, in the case of GaSe and GaS, O atoms create valence bonds with Ga atoms from the atomic planes inside stratified packages, while O atoms adsorbed on the GaTe surface engender valence bonds with the atomic plane outside stratified package.

4. CONCLUSIONS

Optical reflection and transmission in specially undoped and Cu light-doped GaS, GaTe and GaSe single crystal plan-parallel plates, with thickness between 3 μm and ~1.2 mm, in the spectral range 360 nm−~120 μm, was investigated. From the interference analysis of liniar polarized light, dispersion of refractive indices for GaSe(n_e) and GaSe and GaS(n_o) in the range between ~400 nm up to 20–22 μm has been determined. In the energy range $h\nu < E_g$, optical functions $n_o(\lambda)$ and $n_e(\lambda)$ are described by power-type polynomials. In this spectral range, GaSe, GaSe:Cd and GaSe:Cu single crystal samples exhibit $n_o > n_e$ values.

The fundamental absorption edge in GaSe crystals is formed by exciton absorption. The binding exciton energy is equal to 22.6 meV. The direct band gap of GaSe at 293 and 78 K is of 2.035 eV and 2.121 eV, respectively. From the analysis of the absorption edge contour energy of the impurity acceptor level induced by Cd and Cu doping atoms has been determined as 0.14 meV with respect to the valence band top.

The layered crystal structure of III–VI materials determines the anisotropy of the optical absorption in these compounds. At photon energies $h\nu > E_g$, the absorption coefficient for the $\vec{E} \parallel \vec{C}$ polarization is more than 15 times greater than that corresponding to the $\vec{E} \perp \vec{C}$ polarization.

In the photon energy range $h\nu < E_g$, optical spectra of GaS, GaSe and GaTe are determined by the mono- and multiphonon absorptions. From the analysis of the absorption spectra in micrometer-size samples, and of the reflection spectra in samples that no display interference effects, energies of fundamental LO and TO phonons for $\vec{E} \parallel \vec{C}$ and $\vec{E} \perp \vec{C}$ polarizations have been determined. Diphonon reflection and absorption bands in GaSe and GaS layered materials have been identified.

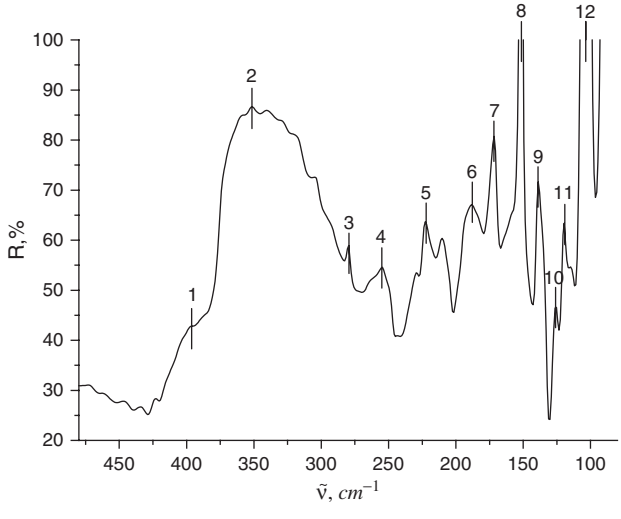

Fig. 17. Reflection spectrum of the oxidized surface of single crystal TeO_2 plate (optical axis parallel to the sample surface).

References and Notes

1. N. Okamoto, T. Takahashi, and H. Tanaka, *Appl. Phys. Lett.* 73, 794 (**1998**).
2. N. Okamoto and H. Tanaka, *Materials Science in Semiconductor Processing* 2, 13 (**1999**).
3. Z. R. Dai, S. R. Chegwidden, L. E. Rumaner, and F. S. Ohuchi, *J. Appl. Phys.* 85, 2603 (**1999**).
4. J. A. Adams, A. A. Bostwick, F. S. Ohuchi, and M. A. Olmstead, *Appl. Phys. Lett.* 87, 1 (**2005**).
5. M. S. Brodin and I. V. Blonskii, Exciton Processes in Layered Crystals, Naukova Dumka, Kiev, (**1986**), (in Russian).
6. A. Kuhn, A. Chevy, and R. Chevalier, *Phys. Stat. Sol. A* 31, 469 (**1975**).
7. G. L. Beleńkiĭ, E. Yu. Salaev, and R. A. Suleimanov, *Sov. Phys. Usp.* 31, 434 (**1988**).
8. M. Schlüter, *Il Nuovo Cimento B Series 11* 13, 313 (**1973**).
9. A. Rizzo, C. de Blasi, M. Catalano, and P. Cavaliere, *Phys. Stat. Sol. A* 105, 101 (**1988**).
10. Z. D. Kovalyuk, O. A. Politanska, O. N. Sydor, and V. T. Maslyuk, *Semiconductors* 42, 1292 (**2008**).
11. Z. D. Kovalyuk, V. N. Katerynchuk, O. A. Politanska, O. N. Sydor, and V. V. Khomyak, *Technical Physics Letters* 31, 359 (**2005**).
12. I. I. Grygorchak, A. I. Pelekhovych, and N. V. Volynskaya, *Semiconductors* 42, 375 (**2008**).
13. S. Shigetomi and T. Ikari, *Jpn. J. Appl. Phys., Part 1* 44, 7521 (**2005**).
14. Z. D. Kovalyuk, O. N. Sydor, V. N. Katerinchuk, and V. V. Netyaga, *Semiconductors* 41, 1056 (**2007**).
15. S. I. Drapak, S. V. Gavrylyuk, Z. D. Kovalyuk, and O. S. Lytvyn, *Semiconductors* 42, 414 (**2008**).
16. S. I. Drapak and Z. D. Kovalyuk, *Technical Physics Letters* 27, 755 (**2001**).
17. B. S. Razbirin, V. P. Mushinskii, M. I. Karaman, A. N. Starukhin, and E. M. Gamarts, *Fiz. Tverd. Tela (St. Petersburg)* 17, 2124 (**1975**).
18. E. Kress-Rogers and R. J. Nicholas, *J. Phys. C: Solid State Physics* 16, 2439 (**1983**).
19. E. J. Johnson, Optical properties of III–V compounds, Semiconductors and Semimetals, edited by R. K. Willardson and A. C. Beer, Academic Press, New York and London (**1967**), Vol. 3, p. 169.
20. R. Le Toullec, N. Piccioli, N. Mejatty, and M. Balkanski, *Il Nuovo Cimento B Series 11* 38, 159 (**1977**).
21. D. S. Gerber and G. N. Maracas, *IEEE J. Quant. Electron* 29, 2589 (**1993**).
22. J. L. Pankove, Optical Processes in Semiconductors, Prentice-Hall, Inc. Englewood Cliffs, New Jersey (**1971**), p. 107.
23. T. A. McMath and J. C. Irwin, *Phys. Stat. Sol. A* 38, 731 (**1976**).
24. K. L. Vodopyanov and L. A. Kulevskii, *Optics Communications* 118, 375 (**1995**).
25. M. A. Hernández, M. V. Andrés, A. Segura, and V. Muñoz, *Optics Communications* 118, 335 (**1995**).
26. M. Schlüter, J. Camassel, S. Kohn, J. P. Voitchovsky, Y. R. Shen, and M. L. Cohen, *Phys. Rev. B* 13, 3534 (**1976**).
27. Y. P. Varshni, *Physica* 34, 149 (**1967**).
28. G. L. Belen'kii and V. B. Stopachinskii, *Sov. Phys. Usp.* 26, 497 (**1983**).
29. I. Evtodiev, *Moldavian Journal of the Physical Sciences* 1, 52 (**2002**).
30. N. B. Mustafaev and N. B. Mustafaev, *Thin Solid Films* 324, 159 (**1998**).
31. S. Jandl, J. L. Brebner, and B. M. Powell, *Phys. Rev. B* 13, 686 (**1976**).
32. V. P. Savchyn and V. B. Kytsai, *Thin Solid Films* 361, 123 (**2000**).
33. Z. D. Kovalyuk, V. M. Katerynchuk, A. I. Savchuk, and O. M. Sydor, *Mater. Sci. Eng., B: Solid-State Materials for Advanced Technology* 109, 252 (**2004**).
34. O. A. Balitskii, R. V. Lutsiv, V. P. Savchyn, and L. M. Stakhira, *Mater. Sci. Eng., B* B56, 5 (**1998**).
35. M. Hass, Lattice Reflection, Semiconductors and Semimetals, edited by R. K. Willardson and A. C. Beer (**1967**), Vol. 3, pp. 13–27.
36. S. Isawa, L. Balsley, and E. Burstein, *Proc. 7th Physics of Semiconductors: Intern. Conf.*, Paris-New York (**1964**), p. 1077.
37. M. Hass and B. W. Henvis, *J. Phys. Chem. Solids* 23, 1099 (**1962**).
38. N. Kuroda and Y. Nishina, *Phys. Rev. B* 19, 1312 (**1979**).
39. E. Finkman and A. Rizzo, *Solid State Commun.* 15, 1841 (**1974**).

Received: 22 June 2011. Accepted: 15 July 2011.